

# Kinetics of photocatalytic degradation of phenols with multiple substituent groups

M.H. Priya, Giridhar Madras\*

*Department of Chemical Engineering, Indian Institute of Science, Bangalore, Karnataka 560012, India*

Received 30 June 2005; received in revised form 13 August 2005; accepted 13 August 2005

Available online 13 September 2005

## Abstract

The photocatalytic degradation of seven phenols, substituted with two of the following groups: chloro, methyl and nitro, was investigated using combustion-synthesized catalyst. The intermediates were analyzed and a possible pathway of degradation was proposed. The first order kinetic rate constants for the degradation of various phenols were determined. The rate of photocatalytic degradation followed the order: 4-chloro,3-methyl phenol > 2-chloro,4-methylphenol > 4-chloro,2-nitrophenol > 4-chloro,2-methyl phenol > 4-chloro,3-nitrophenol ~ 2-chloro,4-nitrophenol > 4-methyl,2-nitrophenol. The overall degradation rate of 4-chloro,3-methyl phenol was nearly an order of magnitude faster than the degradation rate of 4-methyl,2-nitrophenol. Chloromethylphenols degraded faster than chloronitrophenols due to the ring deactivating characteristic of nitro group for hydroxyl radical attack. The nature of substituent groups plays a more important role than the position of the substituent groups in determining the degradation rate of multi-substituted phenols.

© 2005 Elsevier B.V. All rights reserved.

**Keywords:** Photodegradation; Phenols; Substituted phenols; Degradation pathways and mechanisms

## 1. Introduction

Photocatalysis is a promising technology to treat contaminated water. Upon incidence of photon with an energy equivalent or exceeding the band gap energy of the semiconductor photocatalyst, excitation of electron occurs from valence band to conduction band leaving a positive hole in the valence band [1]. Free radicals are generated when positive holes react with hydroxyl species or any electron donor adsorbed at the surface of the catalyst. These highly reactive free radicals oxidize the hazardous pollutants present in the system to CO<sub>2</sub> and H<sub>2</sub>O.

Phenolic compounds are common pollutants that are present in industrial wastewater and therefore, extensive studies have been reported on the photocatalytic degradation of phenols. The influence of various process parameters like temperature [2,3], pH [4–6], initial concentration of pollutants [7–9], light intensity [10,11], presence of anions [3,4] and cations [12,13] has been investigated. The effect of immobilized/suspended

catalyst [2,14–16], and catalyst concentration [17] on photocatalytic degradation of pollutants has also been studied. The type and number of substituent group and its position influence the degradation rate [7,8,18–20]. The effect of substitution and process parameters has been investigated for degradation of chlorophenols [1,8,9,18–26], nitrophenols [7,15,27–32] and cresols [30,33–35].

The industrial effluent is a mixture of various organic and inorganic compounds, which may react to yield compounds with multiple substituent groups. To the best of our knowledge, no study has reported the degradation of such multi-substituted compounds. The usual commercial catalyst used for photocatalysis is Degussa P-25 TiO<sub>2</sub>. However, combustion-synthesized TiO<sub>2</sub> was reported to be more effective catalyst compared to Degussa P-25 for the degradation of chlorophenol [8] and nitrophenol [7,9]. The higher activity of this catalyst compared to that of the commercial Degussa P-25 catalyst [36] is attributed to its smaller size (8–10 nm), lower band gap energy, larger surface area and higher bounded hydroxyl content.

Therefore, the objective of the work was to investigate the degradation kinetics of seven multi-substituted phenols using combustion-synthesized catalyst. The effect of nature of substitution (-chloro, -nitro, and -methyl) and its position were also

\* Corresponding author. Tel.: +91 80 22932321; fax: +91 80 23600683.  
E-mail address: [giridhar@chemeng.iisc.ernet.in](mailto:giridhar@chemeng.iisc.ernet.in) (G. Madras).

examined to understand the influence of substitution on degradation.

## 2. Experimental section

### 2.1. Materials

4-Chloro,3-nitro phenol (4c3n), 2-chloro,4-methyl phenol (2c4m), 2-chloro,4-nitro phenol (2c4n), 4-chloro,2-nitro phenol (4c2n), hydrogen peroxide (Aldrich, USA), 4-chloro,3-methyl phenol (4c3m), nitric acid (S.D. Fine Chemicals Ltd., India), 4-methyl,2-nitro phenol i.e. (4m2n) (Avocado Research Chemicals Ltd., Heysham), 4-chloro,2-nitro phenol i.e. (4c2n) (Alfa Aesar, Heysham), titanium isopropoxide (Lancaster Chemicals, UK), glycine (Merck, India) were used. Water was double distilled and filtered through a Millipore membrane filter prior to use.

### 2.2. Catalyst preparation and characterization

Combustion synthesis technique is a single step process without any downstream processing. Nanosized  $\text{TiO}_2$  was prepared by the solution combustion method using precursor titanyl nitrate  $[\text{TiO}(\text{NO}_3)_2]$  and fuel glycine ( $\text{H}_2\text{N}-\text{CH}_2-\text{COOH}$ ) (all from Merck, India). The titanyl nitrate was synthesized by the reaction of titanyl hydroxide  $[\text{TiO}(\text{OH})_2]$  obtained by the hydrolysis of titanium isopropoxide  $[\text{Ti}(i\text{-OPr})_4]$  (Lancaster) with nitric acid. In a typical combustion synthesis, a Pyrex dish ( $300\text{ cm}^3$ ) containing an aqueous redox mixture of stoichiometric amounts of titanyl nitrate (2 g), glycine (0.8878 g) in 15 mL of water was introduced into the muffle furnace preheated to  $350^\circ\text{C}$ . The solution initially undergoes dehydration and a spark appears at one corner which spreads throughout the mass, yielding anatase titania. In this system, the combustion reaction was of smoldering type without any flame, just a spark appears at a corner and spreads over the mass yielding highly porous nano-sized yellowish substance, pure anatase  $\text{TiO}_2$ . Phase transition to other phases like rutile or brookite is prevented in this process because the material is exposed to very high temperature ( $>900^\circ\text{C}$ ) only for a short duration. This method also involves the liberation of large volume of the gases nearly seven times the moles of the catalyst, which leads to the high porosity and high surface area of the material.

The catalyst was characterized by various methods as discussed below. The X-ray diffraction (XRD) patterns of catalysts were recorded on a Siemens D-5005 diffractometer using  $\text{Cu K}\alpha$  radiation with a scan rate of  $2^\circ\text{ min}^{-1}$ . The XRD pattern of combustion-synthesized  $\text{TiO}_2$  was recorded in  $2\theta$  range from  $5$  to  $100^\circ$ . The pattern can be indexed to pure anatase phase of  $\text{TiO}_2$  with the space group of  $I4_1/amd$ . The data were then refined using Fullprof-98 program. The observed, calculated and difference X-ray diffraction pattern of  $\text{TiO}_2$  is given in Fig. 1. The figure shows there is a good agreement between calculated and observed pattern. It may be noted that background of the X-ray pattern is flat indicating that  $\text{TiO}_2$  is crystalline. The lattice parameter for  $\text{TiO}_2$  is  $a = 3.7865(5)\text{ \AA}$  and  $c = 9.5091(1)\text{ \AA}$ . The crystallite size was determined from XRD pattern using Sherrer

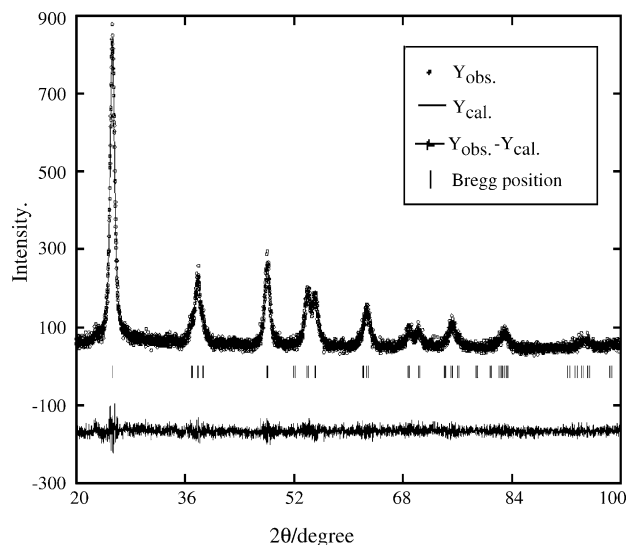


Fig. 1. Observed ( $\circ$ ), calculated (solid line) and difference (bottom) X-ray diffraction pattern of combustion-synthesized  $\text{TiO}_2$ .

formula and based on the full width half maxima (FWHM) of X-ray diffraction pattern, the mean crystallite size is estimated to be  $10 \pm 2\text{ nm}$ .

Transmission electron microscopy (TEM) of powders was carried out using a JEOL JEM-200CX transmission electron microscopy operated at 200 kV. TEM studies also showed the crystallites of  $\text{TiO}_2$  are homogeneous with the mean size of  $8 \pm 2\text{ nm}$ , which agrees well with the XRD measurements. The surface area of the catalyst was determined with standard BET apparatus (NOVA-1000, Quantachrome) and was  $240\text{ m}^2/\text{g}$  and is higher than the surface area of commercial catalysts like Degussa P-25 ( $50\text{ m}^2/\text{g}$ ). Fourier transform infra red (FT-IR) studies were carried out in the  $400\text{--}4000\text{ cm}^{-1}$  frequency range in the transmission mode (Perkin-Elmer, FT-IR-Spectrum-1000) and showed higher surface hydroxyl content for the combustion-synthesized  $\text{TiO}_2$ . The as synthesized  $\text{TiO}_2$  was subjected to thermogravimetric–differential thermal analysis (TG–DTA) (Perkin-Elmer, Pyris Diamond), which showed an 11% weight loss indicating more surface hydroxyl groups. X-ray photoelectron spectra (XPS) of these materials were recorded with ESCA-3 Mark II spectrometer (VG Scientific Ltd., England) using  $\text{Al K}\alpha$  radiation ( $1486.6\text{ eV}$ ). UV–vis absorption spectra of  $\text{TiO}_2$  powders were obtained for the dry pressed disk samples using UV–vis spectrophotometer (GBC Cintra 40, Australia) between 270 and  $800\text{ nm}$  range. The combustion-synthesized  $\text{TiO}_2$  shows two optical absorption thresholds at 570 and  $467\text{ nm}$  that corresponds to the band gap energy of 2.18 and  $2.65\text{ eV}$ , respectively.

Further details on catalyst preparation and characterization are provided elsewhere [7,36,37].

### 2.3. Photochemical reactor

The photochemical reactor employed in the present study is like an annular reactor and has two parts. The reactor consists of a jacketed quartz tube of the following dimensions:  $3.4\text{ cm}$

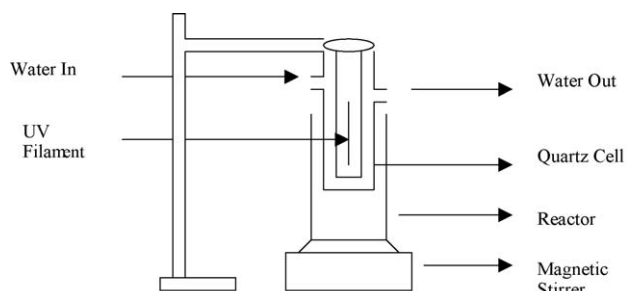


Fig. 2. Schematic of the reactor used for photocatalytic experiments.

i.d., 4 cm o.d., and 21 cm length. This holds a high-pressure mercury vapor (HPML) lamp of 125 W (Philips, India). This is placed in a Pyrex glass outer reactor with dimensions of 5.7 cm i.d. and 16 cm height. Fig. 2 is the schematic diagram of the reactor. The ballast and capacitor were connected in series with the lamp to avoid the fluctuations in the input supply. The solution was taken in the outer reactor and stirred uniformly using a magnetic stirrer during the course of reaction. The excess heating due to dissipative loss of the UV energy was constantly removed using water circulated through the annulus of the jacketed quartz tube. Further details on the operation of the reactor and range of energy emission are given elsewhere [36]. The light source was concentrically placed inside the quartz cell and predominantly emitted the wavelength 365 nm corresponding to the energy of 3.4 eV and photon flux is  $5.8 \times 10^{-6}$  mol photon/s. The pre-weighed amounts of catalyst was added to the solution and maintained in suspension using magnetic stirring in the reactor.

#### 2.4. Degradation experiments

A predetermined amount of substituted phenol was dissolved in double distilled and Millipore filtered water. A catalyst loading of 1 g/L was used for the entire study. Prior to UV irradiation, the catalyst loaded solution was stirred for 30 min in dark to allow the system to attain adsorption–desorption equilibrium. Subsequently, the solution was exposed to UV radiation and samples were taken at regular intervals.

#### 2.5. Sample analysis

The UV absorption spectrum of chloro-methylphenol showed maximum absorbance at  $\lambda$  at 280 nm while that of chloro-nitrophenols and nitro-cresol showed two absorbance peaks corresponding to  $\lambda$  at 280 and 340 nm. Because, the intermediates would interfere with UV absorbance of the parent compound, HPLC analysis was considered appropriate to analyze the samples. Samples, collected at regular intervals, were filtered through Millipore membrane filters and centrifuged to remove the catalyst particles prior to analysis. The HPLC consisted of an isocratic pump (Waters 501), a Rheodyne injector, C-18 column, UV detector (Waters 2487) and a data acquisition system. The eluent stream consisted of 80 vol.% water, and 20 vol.% acetonitrile pumped at 0.8 mL/min. Samples were injected in a Rheodyne valve with a sample loop of 50  $\mu$ L and the UV

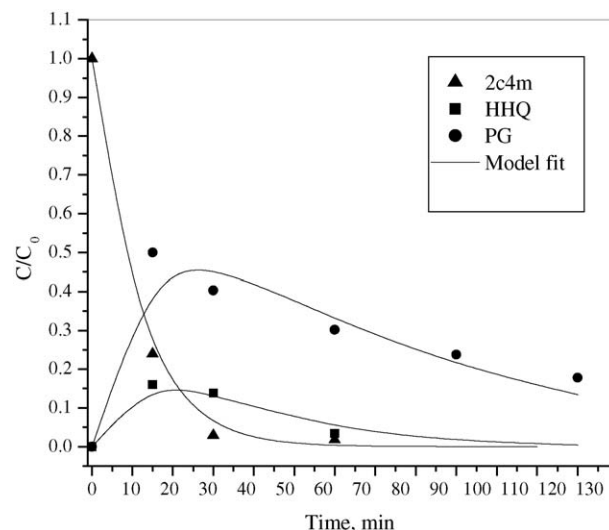


Fig. 3. Normalized concentration profiles of the parent compound and its intermediates observed during the photocatalytic degradation of 80 ppm of 2-chloro,4-methylphenol.

absorbance at 280 nm was continuously monitored using an UV detector and stored digitally. The chromatographic areas were converted to concentration values using calibration curves based on pure compounds.

#### 2.6. Results and discussion

There was no appreciable degradation of the substituted phenols with either UV or catalyst alone. As a catalyst loading of 1 kg/m<sup>3</sup> was found to be the optimum for degradation of various phenolic compounds [8,9], the same catalyst loading was used for the present study. All compounds were stirred in dark for 30 min prior to UV irradiation and no significant decrease in the concentration was observed due to adsorption. In Figs. 3–9, the degradation profiles of seven compounds using combustion-

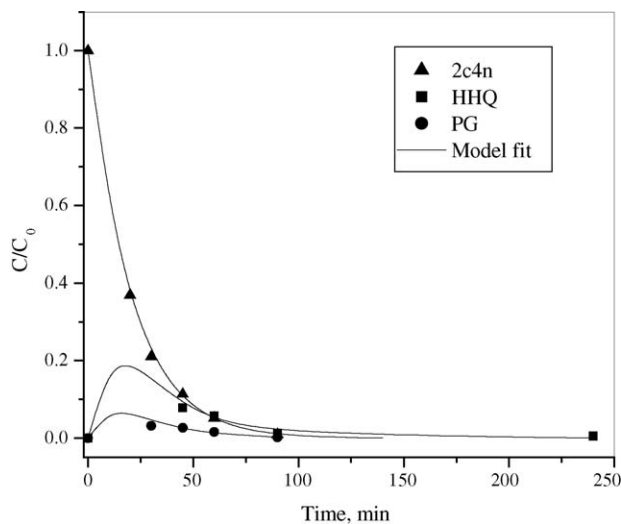


Fig. 4. Normalized concentration profiles of the parent compound and its intermediates observed during the photocatalytic degradation of 75 ppm of 2-chloro,4-nitrophenol.

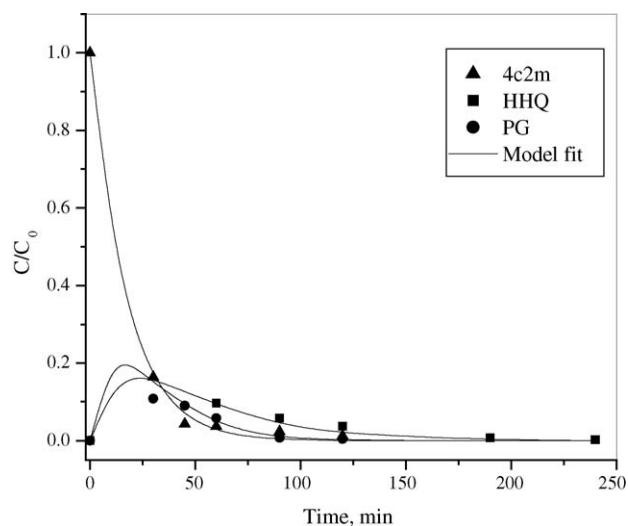


Fig. 5. Normalized concentration profiles of the parent compound and its intermediates observed during the photocatalytic degradation of 75 ppm of 4-chloro,2-methylphenol.

synthesized catalyst are shown along with the concentration profiles of intermediates formed, where  $C$  is the concentration of the compound at time  $t$  and  $C_0$  the initial concentration of the parent compound. The parent compounds degraded to 10% of the initial concentration within 1 h of degradation.

The HPLC analysis of the compounds revealed the sequential formation and degradation (concentration profile passed through a maximum) of two common intermediates with an elution time of 200 and 300 s for all seven compounds. This common appearance of the intermediates indicates that the two intermediates were mere  $-OH$  substituted compounds without any chloro, nitro, and methyl substituents. These compounds were detected to be dihydroxy phenols, hydroxy hydroquinone (HHQ) and pyrogallol (PG). In case of degradation of chloronitrophenol, a third intermediate was detected at a elution time of 430 s in

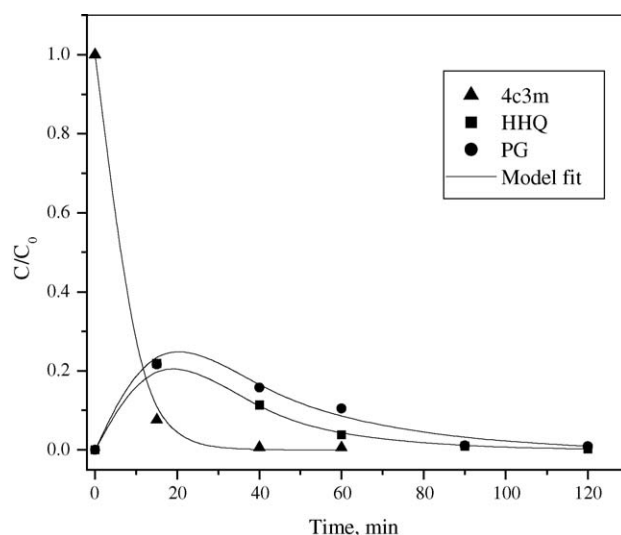


Fig. 7. Normalized concentration profiles of the parent compound and its intermediates observed during the photocatalytic degradation of 75 ppm of 4-chloro,3-methylphenol.

HPLC analysis. In case of degradation of chloromethylphenol (chlorocresol), the third intermediate was observed at an elution time of 540 s in HPLC analysis. It was observed that the maximum concentration of these intermediates occur at an earlier time than that of HHQ and PG indicating that HHQ and PG are degradation products of the third intermediates. Photodegradation of chlorophenol selectively results in hydroquinone over chlorocatechol [8] suggesting that the chloro group of the phenol gets readily replaced by hydroxy group. Therefore, the third intermediate is assumed to be hydroxy nitrophenol and hydroxy cresol, which is obtained by substitution of chloro group by the hydroxyl group in chloronitrophenol and in chloromethylphenol, respectively. Because the simplified mechanism for the degradation of multi-substituted phenols, as discussed below, does not involve the kinetics of formation or decomposition of

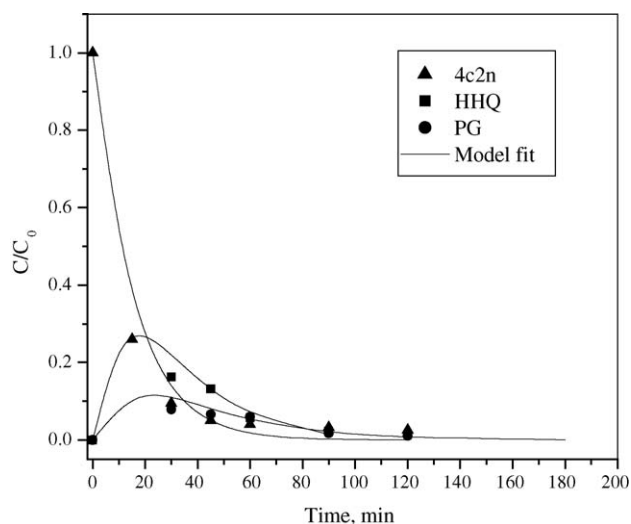


Fig. 6. Normalized concentration profiles of the parent compound and its intermediates observed during the photocatalytic degradation of 80 ppm of 4-chloro,2-nitrophenol.

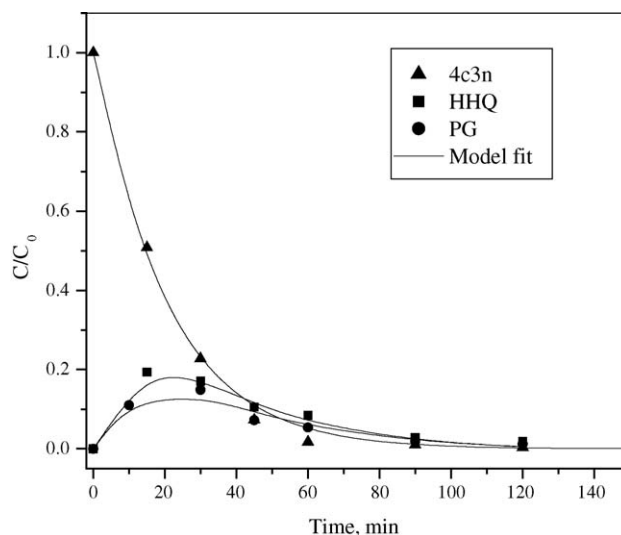


Fig. 8. Normalized concentration profiles of the parent compound and its intermediates observed during the photocatalytic degradation of 75 ppm of 4-chloro,3-nitrophenol.

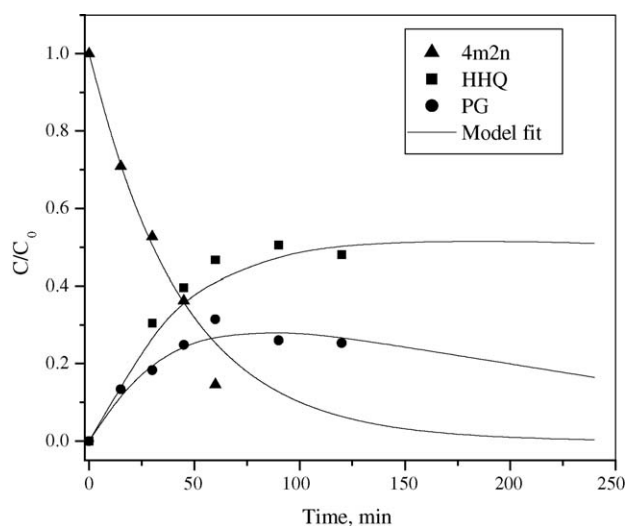


Fig. 9. Normalized concentration profiles of the parent compound and its intermediates observed during the photocatalytic degradation of 75 ppm of 4-methyl,2-nitrophenol.

this intermediate, the intermediate was not quantified by chromatography and, therefore, the degradation of this intermediate is not presented. However, it can be concluded that degradation of multi-substituted phenols follows a sequential replacement of substituents by hydroxy group similar to the degradation of

any substituted phenols. Of the three substituents, replacement of chloro group by hydroxy group occurs more readily than the replacement of other substituents [9]. These replacement processes result in dihydroxyphenols, which could subsequently lead to ring breakage and form organic (linear) acid. Based on above discussion, the postulated mechanism of degradation of multi-substituted phenol is shown in Fig. 10a.

The concentration of primary hydroxylated products like hydroxy nitrophenol and hydroxy methylphenol was low compared to that of HHQ and PG. This observation suggests that the consumption rate of primary hydroxylated compounds is faster than its formation. However, the degradation of secondary hydroxylated compounds (HHQ and PG) is comparatively slower to that of primary hydroxylated products. Thus, it appears that the parent compound directly oxidizes into HHQ and PG.

Therefore, the degradation pathway could be simplified to a simpler mechanism, as shown in Fig. 10b. The kinetic rate constant  $k_1$  is the net equivalent of the rate constants,  $k_{p1}$ ,  $k_{s1}$  and  $k_{s3}$ . The rate constant  $k_2$  can be considered as a composite of kinetic constants,  $k_{p2}$ ,  $k_{s2}$  and  $k_{s4}$ . The degradation rate coefficients,  $k_3$  and  $k_4$ , of the common intermediates (HHQ and PG) are influenced by the presence of primary hydroxylated compounds in the system and, therefore, are different for each phenolic compound. Assuming all reactions to be first order, the rate expression of the parent compound (A), HHQ (B) and PG

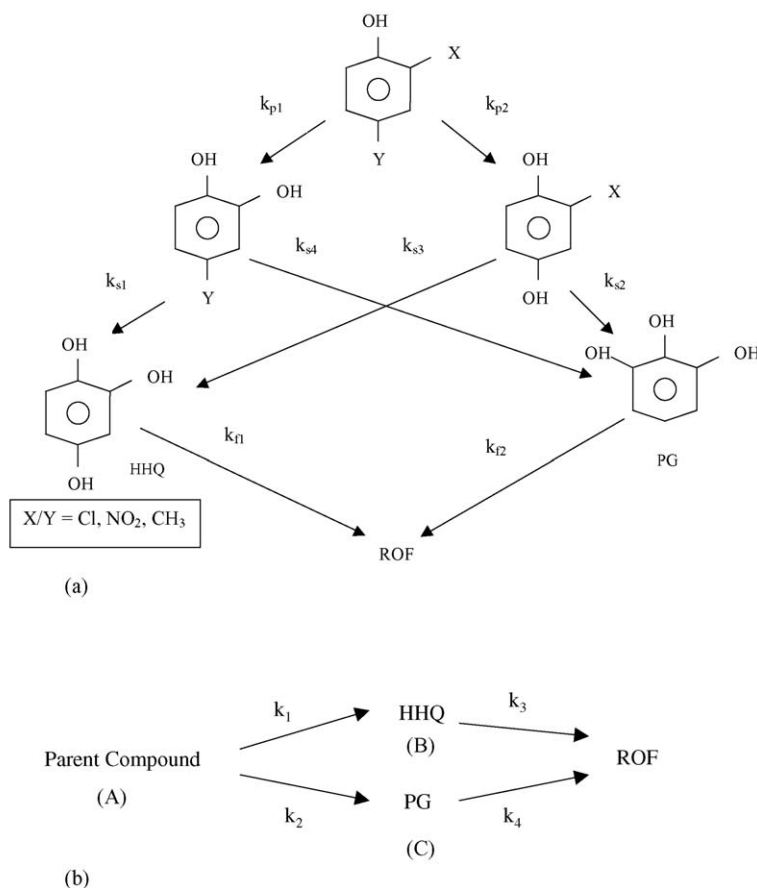


Fig. 10. (a) Postulated mechanism for the degradation of multi-substituted phenols. (b) Simplified mechanism to determine the kinetics.



Table 1

First order kinetic constants ( $\text{h}^{-1}$ ) for photodegradation of multi-substituted phenol

Compound	$k_1$	$k_2$	$k_3$	$k_4$
2-Chloro,4-methylphenol	1.8	3.9	2.4	0.9
2-Chloro,4-nitrophenol	2.1	0.9	4.8	6.6
4-Chloro,2-methylphenol	1.2	2.4	1.8	4.8
4-Chloro,2-nitrophenol	3.0	1.0	3.6	2.3
4-Chloro,3-methylphenol	5.2	5.2	3.0	2.1
4-Chloro,3-nitrophenol	1.8	1.2	3.6	3.1
4-Methyl,2-nitrophenol	0.8	0.6	0.03	0.3

(C) are

$$-\frac{dC_A}{dt} = (k_1 + k_2)C_A \quad (1)$$

$$\frac{dC_B}{dt} = k_1 C_A - k_3 C_B \quad (2)$$

$$\frac{dC_C}{dt} = k_2 C_A - k_4 C_C \quad (3)$$

The linear first order ODEs were solved using Mathematica 4 and non-linearly regressed with experimental data to obtain the kinetic rate constants. The values of the rate constants,  $k_1$ ,  $k_2$ ,  $k_3$  and  $k_4$  are shown in Table 1. The rate of photocatalytic degradation for the parent compound ( $k_1 + k_2$ ) follows the order: 4-chloro,3-methylphenol > 2-chloro,4-methylphenol > 4-chloro,2-nitrophenol > 4-chloro,2-methylphenol > 2-chloro,4-nitrophenol  $\sim$  4-chloro,3-nitrophenol > 4-methyl,2-nitrophenol. In order to verify the proposed degradation mechanism, the degradation of 4-chloro,2-nitrophenol was investigated at four different initial concentrations. The degradation rate coefficients and the degradation profile of the parent compound did not change indicating the validity of the model. The independence of the rate coefficients on the initial concentration confirms that the reactions are first order.

The degradation of 4-chloro,2-nitrophenol is faster than that of 4-methyl,2-nitrophenol, consistent with the earlier observation [8] that chlorophenol degraded faster than methylphenol (cresol). Chloromethylphenol degraded faster than chloronitrophenol, consistent with ring deactivating characteristic of nitro group for hydroxyl radical attack [9]. This is similar to the observation that rate of degradation of methylphenol is higher than that of nitrophenol [30]. It was observed that 4-chloro,3-methylphenol degraded faster than 2-chloro,4-methylphenol, which degraded faster than 4-chloro,2-methylphenol. However, in case of nitrophenol, the degradation rate followed the order: 4-chloro,2-nitrophenol > 2-chloro,4-nitrophenol  $\sim$  4-chloro,3-nitrophenol. The reversal in the order of degradation is attributed to the ring activating and deactivating tendency of methyl and nitro substitution, respectively [9]. Therefore, for multiple substitution, the nature of substituent groups plays a more vital role than the position of the substituent groups in determining the rate of degradation. This is in contrast to the observation [9] that the position of the substituent plays a cru-

cial role in the determination of the photocatalytic degradation of phenols with a single substituent group.

### 3. Conclusion

The photocatalytic degradation of seven multi-substituted phenols was investigated. The organics degraded to 10% of the original concentration within 1 h of degradation. The evolution of intermediates was examined and a probable pathway of degradation was proposed. The reaction followed first order kinetics and the photocatalytic degradation rate coefficients were determined by solving differential equations and regressing it with experimental data. The rate of degradation followed the order: 4-chloro,3-methylphenol > 2-chloro,4-methylphenol > 4-chloro,2-nitrophenol > 4-chloro,2-methylphenol > 2-chloro,4-nitrophenol  $\sim$  4-chloro,3-nitrophenol > 4-methyl,2-nitrophenol. The degradation rate coefficients varied widely depending on the substitution in the phenolic compound. Due to the ring deactivating characteristic of nitro group for hydroxyl radical attack, chloromethylphenols degraded faster than chloronitrophenols. The rate of degradation is primarily determined by the nature of substitution and is less dependent on the position of the substituent group.

### References

- [1] M.R. Hoffmann, S.T. Martin, W. Choi, D.W. Bahnemann, Chem. Rev. 95 (1995) 69.
- [2] W.A. Zeltner, C.G. Hill Jr., M.A. Anderson, Chemtech 23 (1993) 21.
- [3] A.A. Yawalkar, D. Bhatkhande, V.G. Pangarkar, A.A.C.M. Beenackers, J. Chem. Technol. Biotechnol. 76 (2001) 363.
- [4] M. Abdullah, K.C.L. Gray, R.W. Mathews, J. Phys. Chem. 94 (1990) 6620.
- [5] R.W. Mathews, S.R. McEvoy, J. Photochem. Photobiol. A: Chem. 64 (1992) 231.
- [6] M. Trillas, J. Pearl, X. Donenach, J. Chem. Technol. Biotechnol. 67 (1996) 237.
- [7] K. Nagaveni, G. Sivalingam, M.S. Hedge, G. Madras, Environ. Sci. Technol. 38 (2004) 1600.
- [8] G. Sivalingam, M.H. Priya, G. Madras, Appl. Catal. B: Environ. 51 (2004) 67.
- [9] M.H. Priya, G. Madras, J. Photochem. Photobiol. A: Chem. 178 (2006) 1–7.
- [10] K. Okamoto, Y. Yamamoto, H. Tanaka, A. Itaya, Bull. Chem. Soc. Jpn. 58 (1985) 2023.
- [11] D.F. Ollis, E. Pellizzetti, N. Serpone, Environ. Sci. Technol. 25 (1991) 1523.
- [12] T.Y. Wei, Y.Y. Wang, C.C. Wan, J. Photochem. Photobiol. A: Chem. 53 (1990) 115.
- [13] A. Scalfani, L. Palmisano, E. Davi, J. Photochem. Photobiol. A: Chem. 56 (1991) 113.
- [14] R.W. Mathews, S.R. McEvoy, Solar Energy 49 (1992) 507.
- [15] Y. Gao, H. Liu, Mater. Chem. Phys. 92 (2005) 604.
- [16] Y.V. Kolenko, A.V. Garshev, B.R. Churagulov, S. Boujday, P. Portesand, C. Colbeau-Justin, J. Photochem. Photobiol. A: Chem. 172 (2005) 19.
- [17] R.W. Mathews, S.R. McEvoy, J. Photochem. Photobiol. A: Chem. 66 (1992) 355.
- [18] J.C. D'liveira, C. Minero, E. Pelizzetti, P. Pichat, J. Photochem. Photobiol. A: Chem. 72 (1993) 261.
- [19] T. Pandiyan, O.M. Rivas, J.O. Martinez, G.B. Amezcua, M.A. Martinez-Carrillo, J. Photochem. Photobiol. A: Chem. 146 (2002) 149.

- [20] E. Kusvuran, A. Samil, O.M. Atanur, O. Erbatur, *Appl. Catal. B: Environ.* 58 (2005) 211.
- [21] K.H. Wang, Y.H. Hsieh, M.Y. Chou, C.Y. Chang, *Appl. Catal. B: Environ.* 21 (1998) 1.
- [22] D. Chen, A.K. Ray, *Appl. Catal. B: Environ.* 23 (1999) 143.
- [23] J. Bandara, J.A. Mielczarski, A. Lopex, J. Kiwi, *Appl. Catal. B: Environ.* 34 (2001) 321.
- [24] S. Antonaraki, E. Androulaki, D. Dimotikal, A. Hiskia, E. Papaconstantiou, *J. Photochem. Photobiol. A: Chem.* 148 (2002) 191.
- [25] M. Pera-Titus, V. Garcia-Molina, M.A. Banos, J. Gimenez, S. Esplugas, *Appl. Catal. B: Environ.* 47 (2004) 219.
- [26] D. Shchukin, S. Poznyak, A. Kulak, P. Pichat, *J. Photochem. Photobiol. A: Chem.* 162 (2004) 423.
- [27] V. Augugliaro, L. Palmisano, M. Schiavello, A. Sclafani, *Appl. Catal.* 69 (1991) 323.
- [28] M.S. Dieckmann, K.A. Gray, *Water Res.* 30 (1996) 1169.
- [29] V. Maurino, C. Minero, E. Pelizzetti, P. Piccinini, N. Serpone, H. Hidaka, *J. Photochem. Photobiol. A: Chem.* 109 (1997) 171.
- [30] K.H. Wang, Y.H. Hsieh, L.J. Chen, *J. Hazard. Mater.* 59 (1998) 251.
- [31] J. Lea, A.A. Adesina, *J. Chem. Technol. Biotechnol.* 76 (2001) 803.
- [32] M. Ksibi, A. Zemzemi, R. Boukchina, *J. Photochem. Photobiol. A: Chem.* 159 (2003) 61.
- [33] B. Pal, M. Sharon, G. Nogami, *Mater. Chem. Phys.* 59 (1999) 254.
- [34] R.I. Olariu, B. Klotz, I. Barnes, K.H. Becker, R. Mocanu, *Atmos. Environ.* 36 (2002) 3685.
- [35] A. Hatipoglu, N. San, Z. Cinar, *J. Photochem. Photobiol. A: Chem.* 165 (2004) 119.
- [36] G. Sivalingam, K. Nagaveni, M.S. Hedge, G. Madras, *Appl. Catal. B: Environ.* 45 (2003) 23.
- [37] K. Nagaveni, G. Sivalingam, M.S. Hedge, G. Madras, *Appl. Catal. B: Environ.* 48 (2004) 83.